RE-ANALYSIS OF GOME/ERS-2 DIFFUSER PROPERTIES

Sander Slijkhuis[(1)], Sandra Wahl[(1)], Bernd Aberle[(1)], Diego Loyola[(1)]

[(1)]Deutsches Zentrum fuer Luft- und Raumfahrt ,
Remote Sensing Technology Institute (DLR-MF), Oberpfaffenhofen,
82234 Wessling, Germany
Email: Sander.Slijkhuis@dlr.de

ABSTRACT

In this paper, we present results from a study on seasonal dependence of the BSDF. Our study can be divided in two parts. First, we closely follow a method used previously in the GDAQI project. Here the main problem in the analysis is removed by smoothing the data over wavelength. It is found that the BSDF as function of illumination angle is not the expected parabola, but has a plateau (channels 1 & 2) or even a pronounced dip (channels 3 & 4) at the angle where maximum reflectivity was expected.

In the second part we derive a BSDF for each wavelength, which can only be done for channels 1,3,4 but not for channel 2. This leads to the surprising result that the seasonal dependence of the BSDF is not, as expected, a smooth function of wavelength, but shows large (up to 2%) etalon-like variations with wavelength.

1. INTRODUCTION

Trace-gas profile retrievals from the GOME instrument are made by comparing model calculations of atmospheric transmission and backscattering to the observed ratio of Earthshine Radiance to incident Irradiance. In the GOME instrument, the latter is observed once a day by making Solar measurements with a diffuser in the lightpath. The ratio Radiance/Irradiance is thus, in principle, only determined by the Bi-directional Scattering Distribution Function (BSDF) of the diffuser - an absolute radiance calibration of the instrument is not necessary.

In practice, the situation may be more complex: the Irradiance measurements are performed at a different scan mirror angle than the Radiance measurements, which may invoke artefacts due to the instrument's polarisation sensitivity, or due to scan-angle dependent degradation. Furthermore, it has been observed that changing interference patterns arise with changing illumination conditions of the diffuser [1][2] - it is unclear if these features arise only from the diffuser or if they are an interplay between beam-filling effects and interference layers in the main spectrometer.

In this paper, we present results from a study on seasonal dependence of the BSDF. We have used the variablility in the irradiance measurements (corrected for Sun-Earth distance variations) as a proxy for variability in the ratio Radiance/Irradiance. This is considered valid, as there is no a priori reason why the optical path in the Radiance measurements should change with season: although the incident solar illumination varies over season as function of sub-satellite latitude, nearly all illumination conditions keep occuring somewhere on an orbit.

Our study builds on results obtained by E. Hegels (DLR) in the framework of the GDAQI study [3]. In this previous work, the emphasis was on derivation of the instrument degradation, whereas characterisation of the diffuser BSDF was a necessary by-product of the analysis. For that purpose, it was sufficient to describe the BSDF by a 2nd order polynomial function of the azimuthal incidence angle of the solar irradiance. Note that application of this BSDF, which constitutes a significant improvement from the on-ground calibration, is currently available as option in the GOME Dataprocessor Exctraction software [4].

Close examination of the GDAQI results reveals that, after their correction for BSDF and instrument degradation, seasonal patterns are still recognisable on the irradiance data (herafter, we refer to these corrected data as 'residuals'). This is clearly the case for channels 3 and 4, and may be suspected for channel 1. In channel 2, seasonal dependence in the residuals is not apparent, but here the time-sequence of residuals is dominated by jumps in wave-like patterns on the spectra. These wave-like patterns are changes in the etalon [5]. Especially in channel 2 these changes were frequent, due to a vacuum leak which caused changing of the ice layer on the detector after each switchoff of the instrument. In Annex B.5 of the GDAQI report some further figures are presented, which show for selected wavelength the seasonal dependence of the irradiance and the derived BSDF. Also there it is clear that stable seasonal patterns exist which are not properly described by the current BSDF calibration.

Our study can be divided in two parts. First, we closely follow the method used in GDAQI. Here the main problem in the analysis, which is the changing etalon that dominates the residuals, is removed by smoothing the data over wavelength - hence the derived BSDF is also forced to be a smooth function of wavelength. Improvement on the GDAQI work can be achieved by dropping a few restrictions which were set by the scope of the GDAQI project. In GDAQI, the reference date of the analysis was set to 3 July 1995, but especially in this first phase of GOME operations the instrument was not as stable as in later years. Also, GDAQI was concerned with long-time degradation, but in later years jumps occurred in instrument degradation, which made it difficult to find out the subtle seasonal variations which are present in the data record. In this study, we have the freedom to choose an optimum time window for our analysis, and we can concentrate on the periodic effects in the data without the need of providing a parameterisation of instrument degradation.

In the second part of this study we follow a different concept. Here we derive a BSDF for each wavelength. This can only be done when the changes in etalon are not too pronounced, i.e. for restricted time windows in channels 1,3,4 but not in channel 2.

2. SEASONAL DEPENDENCE OF THE 'SMOOTHED' BSDF

For the analysis we selected a time window of nearly three years, starting in September 1995. During this time, the illumination angle of the Sun on the diffuser changed such that each angle was sampled five times. All analyses are performed on the ratio of solar irradiance spectra relative to the first spectrum.

The change in solar intensity is the product of changes in sun-earth distance, solar output, instrument degradation, change in BSDF, and change in Etalon. The first parameter may be calculated. For the timeframe which we have selected, the other parameters are in the order of magnitude:

- solar output: < 0.3% for wavelengths > 263 nm (apart from Mg II and Ca II region)
- instrument degradation: 15% at 260 nm, 5% at 320 nm
- BSDF: up to 1% deviation expected w.r.t. current calibration
- Etalon changes: up to several %

The dominant factor here is the instrument degradation. However, this varies gradually in time and can to a large extent be fitted with a polynomial function. This is not possible with Etalon. In channel 2, one can observe ca. 30 significant changes in etalon structure from mid-1995 to mid-1998 (see GDAQI report Section 4)). For a given wavelength, every change yields a jump in intensity. As etalon cannot reliably be modelled, these jumps cannot be quantified, even if they can be detected by eye. These jumps conceal the seasonal variation in BSDF on the level which we are looking for. In the data which we show here, we have removed the Etalon by fitting each spectrum with a 3rd order polynomial.

Solar variability was modelled using the SOLAR2000 Research Grade V2.23 empirical solar irradiance model from Space Environment Technologies [6]. The variability in the 115-400 nm range of this model is based on analysis of UARS SOLSTICE and SUSIM data; the current version contains analysis up to the year 2002. The model yields spectra at a resolution of 1 nm in this wavelength range. We used the model in a mode which normalises the intensity to a Sun-Earth distance of 1 AU. To restrict the influence of solar variability on the data analysis, we limited in our study the spectra to wavelengths above 250 nm. In our selected timeframe, this limits errors between 250 and 263 nm to the 1% level. On this variability level, the 13 nm wavelength range at the end of the spectrum does not significantly influence the polynomial wavelength fit. The spectral region around the strongly variable Mg II line was cut out and subsequently filled-in using a parabolic function. The effect of this Mg II removal on the polynomial wavelength fit was very small, though, and could have been omitted.

It was found that within the errors, all seasonal changes could be explained as a function of azimuth angle of solar irradiance onto the diffuser, i.e. no periodic signals were found that didn't correlate with this azimuth angle. This is against the expectation we had at the beginning of the study. The correlation with azimuth angle was found to be surprisingly strong, though much more complex than expected. For this reason, we will present all results of the study as function of solar azimuth angle.

Figs. 1 and 2 on the following page show as function of solar azimuth angle the irradiance, normalised to the irradiance of September 1st, 1995, after removal of changes in Sun-Earth distance, instrument degradation, and Etalon. The various panels show data for a selection of wavelengths in each channel. The plotted spectra are rescaled such that for each wavelength, the average value of the spectra in the azimuth interval [-0.1, 0.1] equals 1. The blue line represents the on-ground calibration of the BSDF, and the red line is a second-order polynomial fit which is calculated like the BSDF correction currently used in the GOME Data Processor Extraction software (this means: it is close to, but not necessary fully identical to, the operationally used BSDF since that was calculated using data from a different time window).

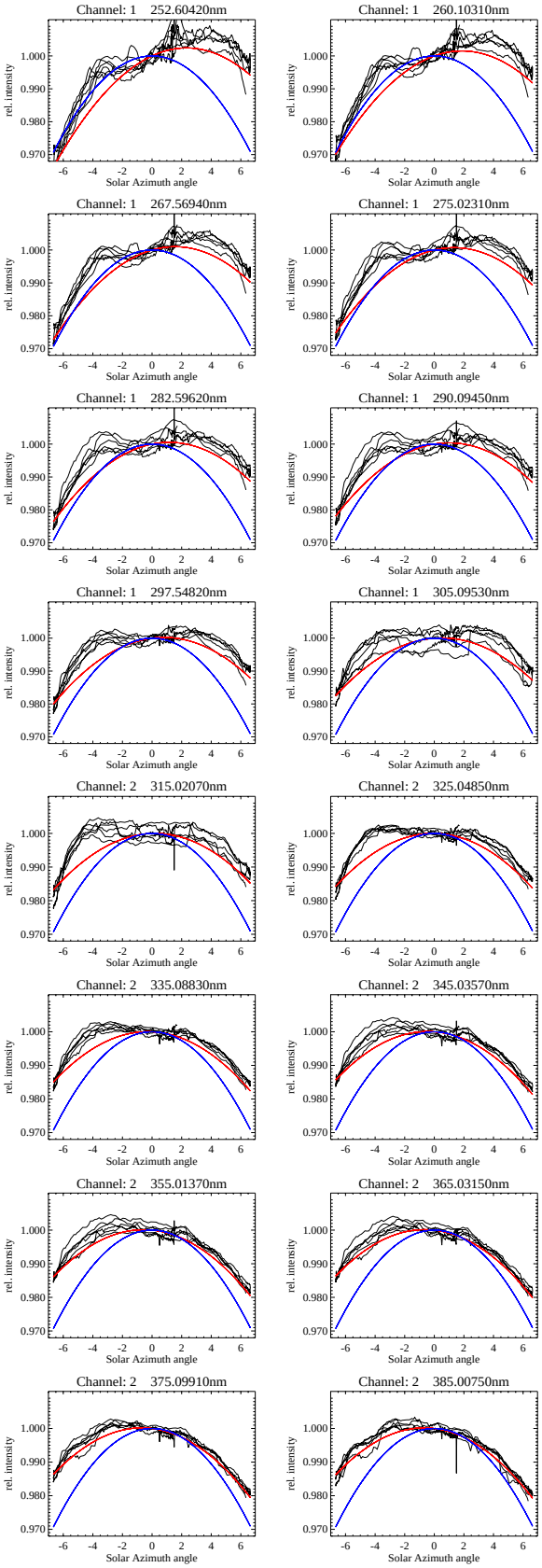

Figure 1: Normalised intensity at 8 wavelengths in channels 1 and 2 as function of solar azimuth angle

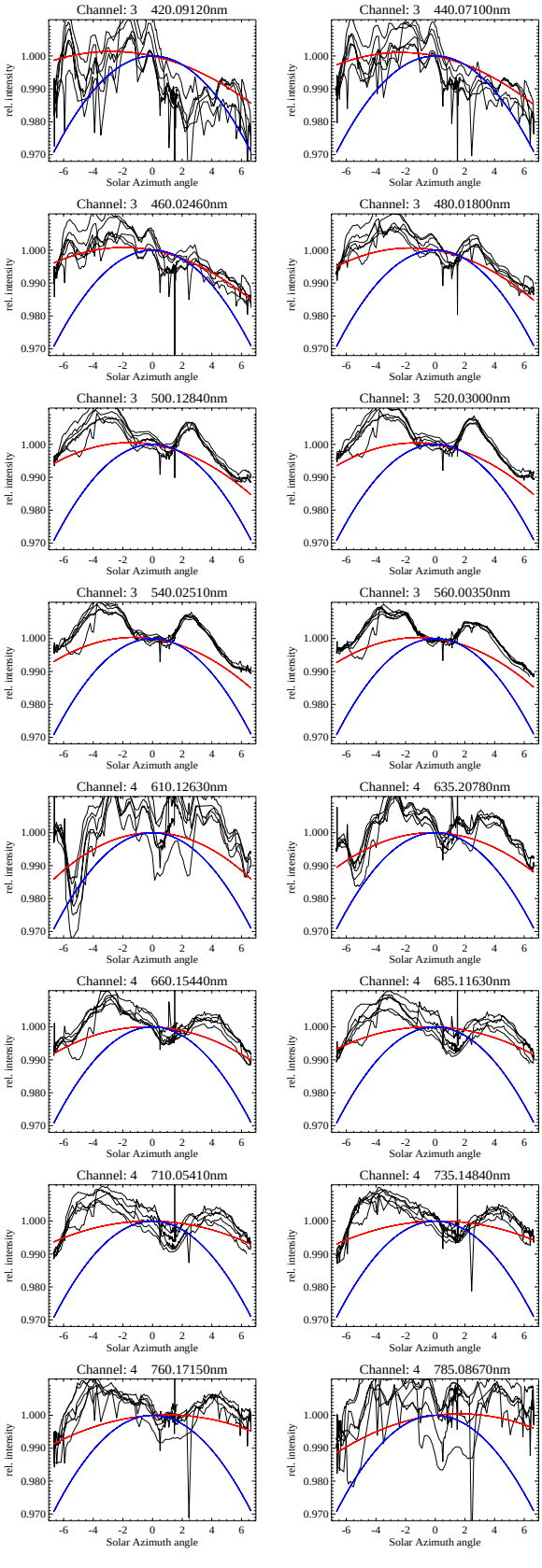

Figure 2: Normalised intensity at 8 wavelengths in channels 3 and 4 as function of solar azimuth angle

The figures show that in channels 1 and 2 the operationally used BSDF performs quite well, except for azimuth angles near -4^o, where deviations up to 1% can be seen. Surprising is that the BSDF is not a monotonous function of incidence angle on the diffuser, but that a pronounced structure is visible reminiscent to 'side-lobe' interference patterns in Fabry-Perot cavities.

The side-lobes have a minimum near 300 nm, and here the BSDF is also the most symmetrical w.r.t. azimuth angle. Note, that as function of wavelength, the curves 'pivot' around azimuth angle 0 (the location of the pivot point may be determined by the normalisation to this angle): for low wavelengths the BSDF is lower for the negative azimuth angles, then becomes symmetrical near 300 nm, and for higher wavelengths the BSDF is lower for the positive azimuth angles. This implies that, cycling over azimuth angle, the spectral shape of the GOME irradiance spectra becomes alternatingly convex and concave over the course of the year.

In channels 3 and 4 the side lobes near azimuth angles of $+/-4^o$ are particularly pronounced. Note also the smaller-scale wobbles on the curves. These features are remarkably reproducible as function of azimuth angle. Even at the beginning of channel 3 and the beginning of channel 4, where the spectra do not overlap in absolute intensity (probably due to dichroic shifts which lift the 3rd order polynomial wavelength fit), the small-scale structure as function of azimuth angle is very similar for all spectra.

3. SEASONAL DEPENDENCE OF THE BSDF WITHOUT WAVELENGTH SMOOTHING

A close look to the residuals plotted in Section 4 of the GDAQI report, shows that for channels 1,3, and 4, the long-term Etalon pattern it quite stable, with a few temporary shifts in Etalon - where after a while the original pattern is restored. On the long term, the Etalon pattern seems to deepen but not to shift with time.

This opens the possibility to derive the seasonal variation in BSDF for each wavelength, without wavelength smoothing. The long-term deepening of the etalon can then be described by a long-term degradation correction which is derived for each wavelength. For a slowly deepening etalon structure, this results in a long-term degradation which is less for wavelengths at the etalon maxima, and stronger for wavelengths in the minima of the etalon curve.

After correction for long-term degradation in this way, one may obtain images which are similar to Figs. 1 and 2, but generally show a larger scatter amongst the BSDF values for subsequent seasons. This is due to the fact that any shifts in etalon cause jumps in the intensity (as function of time) for a particular wavelength. Nevertheless, we can still derive a meaningful fit of BSDF versus solar azimuth angle: the shape of this curve remains well-defined, although the absolute level scatters more as the etalon moves around its average position. This is similar to the dichroic shift problem in the beginning of channel 3 seen in Fig. 2. In fact, for the beginning of channel 3, the scattering now becomes smaller, as the calculation of long-term degradation without wavelength smoothing can compensate for a steady dichroic shift.

In the actual procedure, an iteration loop is used between deriving the BSDF on the assumption of a long-term degradation, and deriving the long-term degradation on the assumption of a BSDF; three iterations are found to be sufficient. Before the iteration starts, high-frequency noise is removed from the (ratio of) spectra - in this sense the derived BSDF will be somewhat smoothed in wavelength. The noise is primarily introduced by the fraunhofer structure because the spectra are not perfectly aligned in wavelength to the reference spectrum. Noise removal is done by low-pass fourier filtering using the same method as the etalon filtering described in [7] (except that the low frequencies are not cut out). The cut-off filter frequencies are chosen from the point where the fourier transform of the summed normalised spectra start to show white noise.

The results for channel 1 are shown in the following two figures. Fig. 3 shows for 8 different azimuth angles the seasonal variation of the BSDF as function of wavelength. The curves have been normalised to the BSDF at azimuth angle 0. The dotted lines represent 3rd order polynomial fits over wavelength for each azimuth angle.

Fig. 4 presents the full 2-dimensional surface of the renormalised BSDF in channel 1: as function of wavelength and as function of solar azimuth angle. Note that a slice in the XZ plane would yield a curve as in Fig. 3, while a slice in the YZ plane would yield a curve like in Fig. 1.

The results for channels 3 and 4 are shown in Fig.5. This plot is similar to Fig. 3.

These results show that there is not just a steady deepening etalon on the solar irradiance data, but the etalon also shows periodic fluctuations as function of illumination angle on the diffuser. In addition, there are periodic, high-frequency wiggles in channels 3 and 4 - this is not surprising in view of studies performed earlier, see e.g. [2].

The question is how reliable the method of determining the 'unsmoothed' BSDF is, i.e. how insensitive it is to changes in Etalon pattern. After all, the changing Etalon patterns may cause significant jumps in intensity for each pixel, and the question is here if the periodic

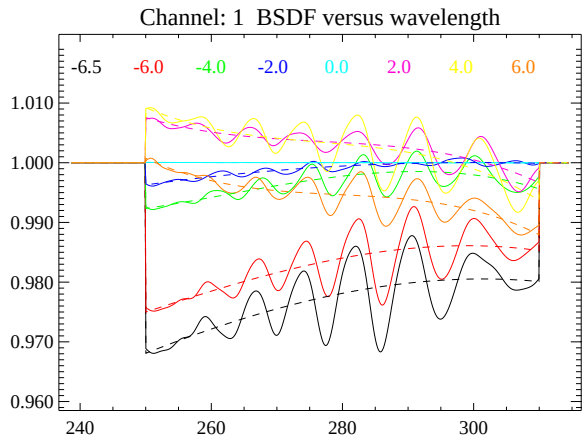

Figure 3: Seasonal variation in BSDF for channel 1, for 8 azimuth angles, normalised to azimuth=0

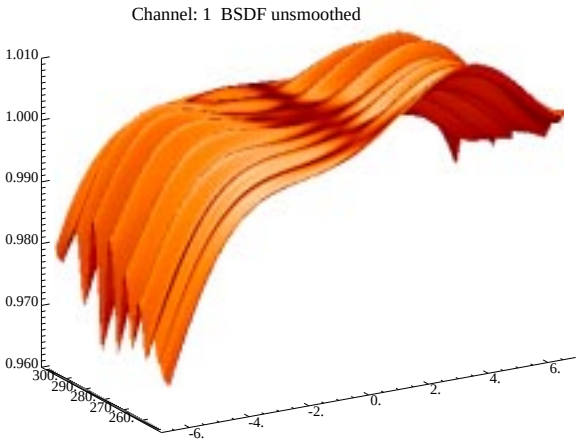

Figure 4: Two-dimensional surface of BSDF for channel 1, as function of azimuth angle (X-axis) and wavelength (Y-axis), normalised to azimuth=0

changes with azimuth are strong enough to be detected despite these jumps.

One test is to see if the method of determining the 'unsmoothed' BSDF yields, after polynomial fitting over wavelength, the same result as the method of determining the 'smoothed' BSDF. The dotted lines in Figs 3 and 5 represent 3rd order polynomial fits over wavelength for each azimuth angle. If the fits are not influenced significantly by shifts in etalon structures, these dotted lines should be identical to the 'smoothed' BSDF from Section 2. This is indeed the case, apart from some small differences at the fit window edges which may be attributed to uncertainties in the polynomial fitting of etalon structures (note that for the 'smoothed' BSDF we fit etalon structures on the measurement spectra, while for the wavelength fit of the 'unsmoothed' BSDF we fit etalon structures on the BSDF).

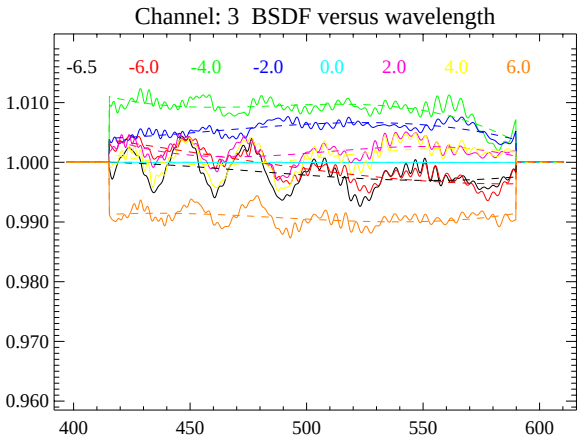

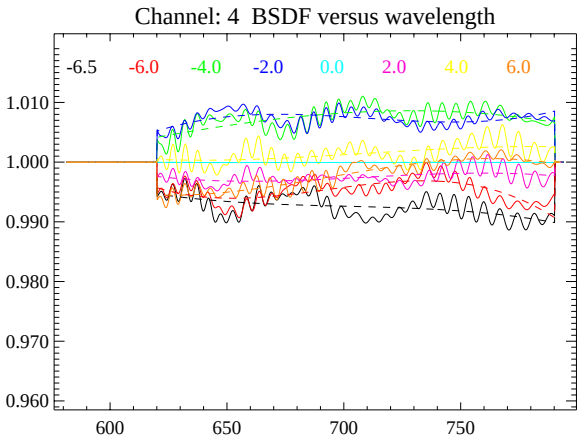

Figure 5: As Fig.3, for channels 3 and 4

Another test is to do the calculations for the 'unsmoothed' BSDF in another time window. For this verification we chose the time interval between June 1996 and June 1999. This shows that for channel 1 the etalon structure is basically the same. The amplitude of the etalon, and also the amplitude of the mean seasonal variation, is slightly larger in this verification time window than in the original calculation. However, the scatter in the relative intensities (due to non-uniform instrument degradation or solar variability) is so much larger here, that the difference is not significant (with relative intensity we mean curves as in Fig. 1). Significant is that the position of the etalon pattern is the same. This is not the case for channel 2, which confirms our expectation that for channel 2 only a 'smoothed' BSDF may be reliably derived. For channels 3 and 4 the verification time window basically yields the same results as the original calculation; also there the scatter in relative intensities is much larger than the difference in derived BSDF.

4. CONCLUSIONS

This work shows two surprising effects in the seasonal variation of the GOME BSDF:

- The BSDF varies not as a simple monotonically increasing or decreasing function of solar azimuth angle, but has ‘sidelobes’ which peak near azimuth angles of $\pm 4°$.
- The BSDF varies not as smooth function of wavelength, but shows a strong etalon feature which varies with solar azimuth angle. Channels 3 and 4 show in addition high-frequency wiggles.

Regarding the azimuth behaviour, the difference with a second order polynomial fit as used in the operational GDP is of the order of $+/-0.5\%$.

A limitation of this study is that we can only derive the spectral structure relative to a reference date or reference azimuth angle. The absolute spectral structure on the ratio irradiance/radiance must be found by other means, but the results from this study may be used to generate a homogeneous level 1 data set where the relative changes are removed.

Acknowlegdement: part of this study was performed under ESA contract for the CHEOPS-GOME project (Climatology of Height-Resolved Earth Ozone Profiling Systems for GOME)

5. REFERENCES

[1] S. Slijkhuis, "GOME instrument properties affecting the calibration of radiance and polarisation", in GOME Geophysical Validation Campaign, ESA WPP-108, 1996

[2] A. Richter and T. Wagner, "Diffuser Plate Spectral Structures and their Influence on GOME Slant Columns", Technical Note, Institut für Umweltphysik Univ. Bremen and Institut für Umweltphysik Univ. Heidelberg, January 2001

[3] I. Aben, M. Eisinger, E. Hegels, R. Snel, C. Tanzi, "GOME Data Quality Improvement GDAQI Final Report", SRON report TN-GDAQI--003SR/2000 < http://www.sron.nl/divisions/eos/external/gdaqi/gdaqi.html >, 29.9.2000

[4] GOME Data Processor - Extraction Software User's Manual, ER-SUM-DLR-GO-0045, Issue 1, 4.8.1999

[5] Jochen Stutz and Ulrich Platt, "Problems in using diode arrays for open path DOAS measurements of atmospheric species", Institut für Umweltphysik, Universität Heidelberg

[6] W. Kent Tobiska et al., The SOLAR2000 empirical solar irradiance model and forecast tool, J. of Atm. and Solar-Terrestial Physics 62, p.1233, 2000

[7] SCIAMACHY Level 0 to 1c Processing - Algorithm Theoretical Basis Document, ENV-ATB-DLR-SCIA-0041, Issue 1, 19.2.1999